Structure and energetics of c-Si/a-SiO_2 systems: Planar interfaces and embedded Si nanocrystals

LingTi Kong and Laurent J. Lewis*

Département de Physique et Regroupement Québécois sur les Matériaux de Pointe (RQMP), Université de Montréal, Case Postale 6128, Succursale Centre-Ville, Montréal, Québec H3C 3J7, Canada

(Received 23 July 2007; revised manuscript received 4 October 2007; published 11 February 2008)

We use Monte Carlo simulations to study the properties of the interfaces between c-Si and a-SiO_2, more specifically planar interfaces and interfaces between a-SiO_2 and embedded Si nanocrystals (NCs). We find that the Si(111)/a-SiO_2 interface with suboxide Si^{+1} only has the lowest interfacial energy among the planar cases considered. We also find that embedded NCs smaller than ~20 Å have even lower interfacial energy, suggesting that a faceted shape is favorable only for large NCs. No significant differences are observed between normal and twinned NCs, indicating that the experimentally observed stacking faults might result from the coalescence of small defect-free NCs.

DOI: 10.1103/PhysRevB.77.085204 PACS number(s): 68.35.Ct, 68.35.Md, 61.46.Hk

I. INTRODUCTION

Because of potential applications in single-electron transistors,[1] memory,[2,3] and light-emitting devices,[4,5] Si nanocrystals (NCs) embedded in amorphous SiO_2 have drawn considerable attention in recent years from both experimental[6–8] and theoretical[9–12] viewpoints. It is generally accepted that the structure and energetics of the interface between the NCs and the amorphous matrix, as well as nearby defects (bonding, chemical, and structural), play an important role in the performance of the devices. It is therefore important to gain a thorough understanding of the properties of the interface between c-Si and a-SiO_2, and this can be achieved using numerical models. Most models to date, however, consider the SiO_2 matrix to be crystalline, which results in huge stresses at the interface.[9,10]

In this paper, we propose a Monte Carlo (MC) scheme for generating realistic composite c-Si/a-SiO_2 models. We use this to study c-Si NCs embedded in a-SiO_2 with and without a twinning layer; we examine their structure and energetics as a function of the NC size, considering first the case of planar interfaces. We find that the Si(111) interface with only Si^{+1} has the lowest energy; we also find that the faceting of embedded c-Si NCs[6,8,13] is driven by the minimization of the interfacial energy and that structural microdefects such as twinning[8,14] in the embedded c-Si NCs result from the coalescence of smaller NCs.

II. COMPUTATIONAL DETAILS

The composite systems are generated by first constructing a pure a-Si model (or more precisely region) using the Wooten-Winer-Weaire (WWW) MC algorithm,[11,12,15] then decorating all Si-Si bonds in this amorphized region with O atoms. The geometry is imposed by requiring selected atoms to remain crystalline: for planar interfaces, appropriate c-Si layers are fixed (depending on the orientation), and for the embedded c-Si NCs, Si atoms within a predetermined radius from the center of the cell are not allowed to move. The WWW method, originally proposed for constructing a-Si continuous random networks, proceeds through sequential bond-switch Monte Carlo moves: at each iteration, a random bond switch is attempted and accepted with probability $\min(1, e^{-\Delta E/k_B T})$, where ΔE is the change in energy resulting from the move. With small modifications, this algorithm can be used for silica.[16] In practice, several optimization steps were invoked in order to speed up the simulations, notably early rejection and local minimization.[16–18]

The energy of the system is approximated by Keating-like potentials,

$$E = \sum_{i \in \text{bonds}} \frac{1}{2} k_i^b (b_i - b_{i0})^2 + \sum_{j \in \text{angles}} \frac{1}{2} k_j^\theta (\cos\theta_j - \cos\theta_{j0})^2, \tag{1}$$

where b_{i0} and θ_{j0} are the equilibrium bond length and bond angle, respectively. We use the parameters proposed in Ref. 16, which have been found to be the most suitable for amorphous SiO_2 among several sets of parameters available.[16] However, since we are studying the composite system of Si and SiO_2, suboxide Si atoms (Si^{+1}, Si^{+2}, and Si^{+3}) will be involved and a suboxide "penalty" energy, which accounts for the chemical energy cost associated with the formation of suboxide atoms, must also be included; these are taken as 0.47, 0.51, and 0.24 eV for Si^{+1}, Si^{+2}, and Si^{+3}, respectively.[11,19] Finally, a repulsive potential between third nearest neighbors and beyond is also needed to prevent nonbonded atoms from overlapping during the simulations. The following simple expression is employed:

$$E_{\text{nonbonded}} = \begin{cases} \frac{1}{2} \sum_{i,j} k_{ij}^r (r_{ij}^2 - r_{ij_0}^2)^2, & r_{ij} < r_{ij0} \\ 0, & r_{ij} \geqslant r_{ij0}, \end{cases} \tag{2}$$

where k^r_{SiSi}=0.4 eV/Å^4, k^r_{SiO}=0.1 eV/Å^4, k^r_{OO}=0.8 eV/Å^4, r_{SiSi_0}=3.84 Å, r_{SiO_0}=2.2 Å, and r_{OO_0}=2.6 Å, respectively. The limited-memory Broyden-Fletcher-Goldfarb-Shanno method[20,21] is employed for the energy minimization. Periodic boundary conditions are applied in all cases.

The preparation of the initial a-Si matrix proceeds by gradually quenching the system from 2.0 to 0.1 eV for a total of $2000n$ trial steps, with n the total number of Si atoms. The highly strained model obtained after introducing the O atoms is then relaxed to minimum energy by adjusting the size of the system along z for planar interfaces, or the total volume for embedded NCs, as well as the coordinates of the atoms, while keeping the crystalline region fixed. A further

WWW quench from 0.5 to 0.1 eV is carried out for another $2000N$ steps, with N the total number of Si and O atoms. Since the computational cost associated with the WWW method scales as N^2, the efficiency of the procedure can be considerably improved by ignoring the O atoms in the first stage of amorphization. In the final quench stage (at 0.1 eV), all atoms are allowed to switch bonds and relax (including the atoms in the c-Si region—this is necessary to allow atoms near the interface to relax completely; elsewhere, they have essentially zero bond-switch probability). The properties are calculated by averaging over the last $100N$ steps at the lowest energy (0.1 eV). During the whole process, the volume of the system is allowed to vary so as to minimize the internal stress. The resulting models are found to be defect-free; in particular, there are no O-O or dangling bonds.

III. RESULTS AND DISCUSSION

A. Planar interfaces

Planar c-Si/a-SiO_2 interfaces with four different c-Si orientations were studied, viz., Si(001), Si(110), Si(111), and Si(112). For flat interfaces, the ionization state of the suboxide Si atoms depends on the orientation and the depth at which O atoms are introduced: for Si(001), the only possible state is Si^{+2}; for Si(110) and Si(111), there are two possibilities, viz., Si^{+1} and Si^{+3}; and for Si(112), both Si^{+2} and Si^{+3} are present, in a ratio of 1:2. (In what follows, the ionization state is indicated in square brackets, e.g., $[Si^{+1}]$.) For all planar interface models, the initial pure Si model has dimensions of $\sim 26\times 26\times 30$ Å^3 [e.g., 7×7 unit cells and 20 layers for Si(001)]; O atoms are introduced in roughly half of the simulation cell in the z direction. Figure 1 presents a typical configuration. For each model, several independent runs were carried out in order to ensure proper statistics; the interfacial energies were evaluated by subtracting the energies of the bulk c-Si and a-SiO_2 phases (obtained in separate calculations) from the total energies of the composite systems.[11,22]

The results of our calculations are presented in Table I. The energy of the Si(111)$[Si^{+1}]$/a-SiO_2 interface is found to be the lowest; next, we have the Si(112) and Si(001)$[Si^{+2}]$ interfaces; Si(110)$[Si^{+3}]$ has the highest energy and is therefore not favored. The Si(111)$[Si^{+3}]$/a-SiO_2 has a relatively high interfacial energy, but this is quite comparable to those of Si(001)$[Si^{+2}]$ and Si(112), suggesting that Si(111) would be the most favorable surface to form an interface with a-SiO_2.

Our results agree with available data from the literature, as can be appreciated in Table I; in particular, they are close to those of Hadjisavvas *et al.*,[12] even though these authors find the Si(001)$[Si^{+2}]$ interface to have the lowest energy among the orientations considered; however, the differences are small—and can probably be viewed as error bars—presumably resulting from differences in the modeling procedure. Our interfacial energies are also found to be of the same order as those from *ab initio* calculations, noting, however, that these are limited in size and both subsystems are assumed to be crystalline.[23]

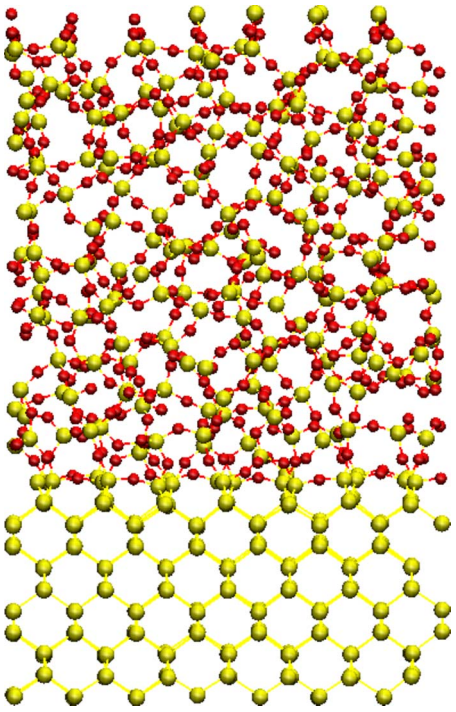

FIG. 1. (Color online) Slice of a ball-and-stick representation of the interface model for Si(001)$[Si^{+2}]$/a-SiO_2. Large (yellow) and small (red) spheres represent Si and O atoms, respectively.

There are very few experimental data to compare with; Wang *et al.*[13] found that the interfacial energies for {100} and {111} were in a ratio of about 1.1, in excellent accord with our calculations which predict 1.13. Otherwise, there have been numerous reports that {111} surfaces are predominantly observed in Si NCs embedded in a-SiO_2,[6,8,13,24] in line with the present prediction of a lowest interfacial energy for (111).

Although the interface structure is not known in detail from experiment, there is strong evidence that all suboxide states of Si are present.[25–27] A model for the Si(001) orientation with suboxides in a $\sim 1:1:1$ proportion was therefore also constructed; this introduce some roughness into the interface. It turns out that its interfacial energy is higher than that of Si(001)$[Si^{+2}]$ (cf. Table I). This is consistent with the experimental observation that Si^{+2} dominates at the Si(001)/a-SiO_2 interface.[25] Likewise, for the Si(111) interface, a suboxide ratio of $\sim 1:1:1$ leads to an energy which is higher than that with Si^{+1} or Si^{+3} only. This is consistent with x-ray photoemission spectroscopy which finds Si^{+1} to be the dominant suboxide on (111).[25,28]

The bonding pattern at the interface—in particular, for the (001) orientation—is of direct relevance to silicon technology. For the Si(001)$[Si^{+2}]$ interface, as can be observed in Fig. 1, nearly all Si atoms in the topmost Si layer are bridged by Si-O-Si bonds, forming a mixture of the so-called "stripe" and "check" phases.[22] When Si^{+1} and Si^{+3} are also present, besides the overwhelming bridging bonds, there is also a notable proportion of Si-Si dimers, a structure often used in interface models.[23,29,30] We also observe that when all suboxide Si atoms are present, Si^{+1} atoms tend to lie within the crystalline region, Si^{+2} at the interface, and Si^{+3} near the amorphous oxide.

TABLE I. Calculated interfacial energies (eV/Å^2) for various planar c-Si/a-SiO_2 interface models, and comparison with other calculations and models.

Si orientation	(001)	(001)	(110)	(110)	(111)	(111)	(111)	(112)
$Si^{+1}:Si^{+2}:Si^{+3}$	0:1:0	~1:1:1	1:0:0	0:0:1	1:0:0	0:0:1	~1:1:1	0:1:2
This work	0.062 ± 0.004	0.078 ± 0.003	0.075 ± 0.002	0.104 ± 0.005	0.055 ± 0.001	0.066 ± 0.003	0.117 ± 0.004	0.062 ± 0.002
Ref. 12	0.046		0.056		0.056			0.051
Ref. 22	0.0068							
Si orientation	(001)	(001)	(001)	(110)	(111)	(111)		
$Si^{+1}:Si^{+2}:Si^{+3}$	1:1:1	1:1:1	1:0:0	1:0:0	1:0:0	1:0:0		
Ref. 23, GGA	0.084	0.090	0.070	0.115	0.099	0.108		
Ref. 23, LDA	0.090	0.096	0.076	0.108	0.096	0.104		

B. Embedded nanocrystals

For c-Si NCs embedded in a-SiO_2, now, two cases were considered, viz., normal spherical and spherical with a twinning layer along the [111] direction. The latter is interesting because it has been observed recently that NCs larger than 6 nm exhibit nanotwinning, while smaller NCs are usually defect-free.[8,14]

The composite systems for the embedded NCs were prepared by excluding the Si atoms within a spherical region of the initial pure Si model from being amorphized and/or oxidized. The latter is set up along the (111) direction and follows the $\cdots ABCABC\cdots$. stacking sequence for the normal NC, and the $\cdots ABCCBA\cdots$ sequence for the twinned NC, the twin interface being located at the center of the system. In addition, the initial model is chosen to be as closely cubic as possible, and such that the thickness of the SiO_2 region between the embedded NC and its images (because of periodic boundary conditions) is always larger than 10 Å. Models with embedded NC from ~1.0 to ~3.5 nm in diameter were thus obtained, corresponding to NCs containing between 26 and ~1200 atoms; the total number of atoms in the system ranged from ~1000 to ~7000. A typical example is presented in Fig. 2.

The interfacial properties are studied as a function of the NC diameter, given by $D=2\Sigma_i r_i/N_{\mathrm{sub}}$, where N_{sub} is the number of suboxide Si atoms and r_i is the distance from suboxide atom i to the center of the NC. The interfacial energy of the composite system is estimated from $\gamma=\Delta E/\pi D^2$, where ΔE is obtained by subtracting the bulk energies of a-SiO_2 and c-Si from the total energy of the composite system. Several independent calculations were carried out and averaged over for each model.

We plot in Fig. 3(a) the dependence of the interfacial energy γ on D. In both cases (normal and twinned), the energy increases roughly linearly up to sizes of 20–25 Å, then it settles to an approximately constant value. There are no significant differences between normal and twinned NCs. Figure 3(b) shows the corresponding variations of the width of the interface, given by the standard deviation of the nominal radius $\bar{r}=D/2$, $\sigma=\sqrt{\Sigma(r_i-\bar{r})^2/N_{\mathrm{sub}}}$.[11] It can also be defined in terms of the distribution of suboxide atoms, i.e., the distance between the first and last suboxide shells along the radial direction d; this is shown in Fig. 3(c). The two definitions are somewhat arbitrary and need not agree; nevertheless, they yield similar trends, as found for the energy, the width increases linearly then saturates above 20–25 Å. The suboxide method provides a converged width of about 2.5 Å, approxi-

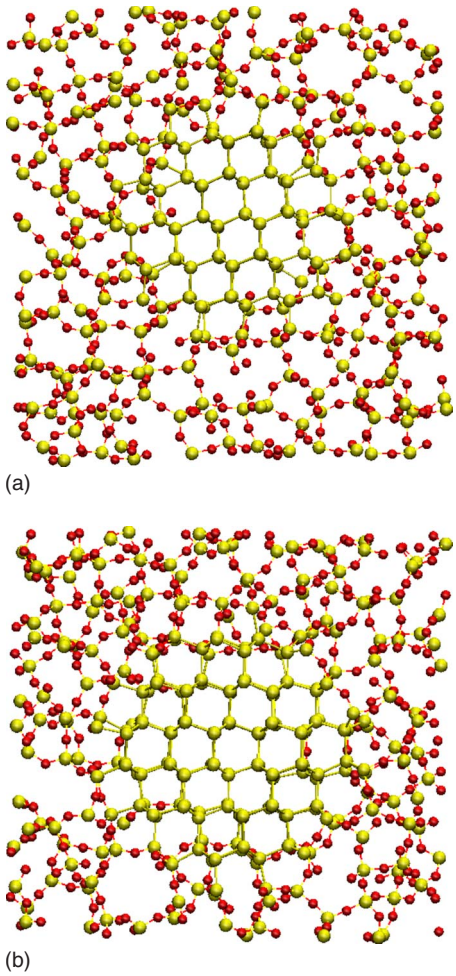

FIG. 2. (Color online) Slices of ball-and-stick representations of (a) a normal, spherical embedded NC and (b) a twinned NC; in both cases, the NC diameter is ~2.0 nm. Large (yellow) and small (red) spheres represent Si and O atoms, respectively.

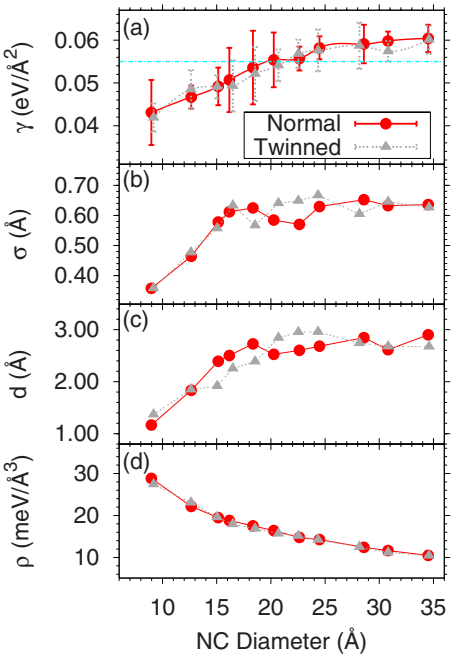

FIG. 3. (Color online) Variation of (a) interfacial energy γ, (b) interfacial width σ, (c) spanning of suboxide Si across the interface d, and (d) excess energy density ρ, with NC diameter. The horizontal dash-dotted line in (a) indicates the interfacial energy for the planar interface of Si(111)[Si^{+1}]SiO_2.

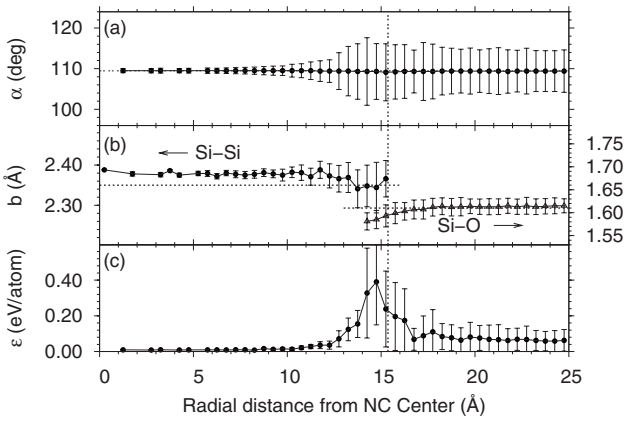

FIG. 4. Radial distribution of (a) bond angle on Si atoms α, (b) Si-Si and Si-O bond lengths b, and (c) average atomic energy ε for a normal, spherical NC of diameter ~30 Å. The vertical dashed line indicates the position of the nominal radius; the horizontal dotted lines in (b) represent the equilibrium Si-Si and Si-O bond lengths. The "error bars" are the standard deviations of the data within the corresponding radial shell.

mately the Si-Si bond length, suggesting an abrupt interface. Again here, normal and twinned NCs behave in the same manner. Evidently, the interface energy is closely related to its width. The present results are at variance with those reported in Ref. 11, where both the energy and the width decrease with size. This is apparently related to the procedure used to generate the models which, according to our calculations, are incompletely relaxed and contain a fair amount of stress; indeed, using the β-cristobalite structure as a starting point (as in Ref. 11), we were able to lower the energy significantly by a more thorough relaxation, especially for small NCs. Evidently, both γ and σ should approach zero at small diameter; for large NCs, the two calculations agree.

The interface with the oxide induces significant distortions in the positions of the atoms. Figure 4 shows the distortion pattern induced by the existence of the interface for an ~30 Å NC. The angles subtended by Si atoms (i.e., Si-Si-Si, Si-Si-O, and O-Si-O) remain close to 109.4° on average but exhibit large variations (~4.5°) as the interface is approached (and passed). Likewise, the Si-Si bond length is slightly stretched over most of the NC, with negligible variations except near the interface. The Si-O bond, in contrast, is slightly compressed near the interface, but rapidly settles to its normal value when moving into the oxide. This is perfectly consistent with x-ray reflectivity results which show the interfacial region to have a higher density than either c-Si or a-SiO_2.[31]

The above results suggest that, in the composite system, strain lies not only at the interface but also within the NC. This finds an echo in the distribution of energy. The total energy can be decomposed into individual atomic contributions by dividing the bond-stretching energy equally between the two bonding atoms, assigning the bond-angle energy to the vertex atom and adding the chemical penalty energy to the suboxide Si atom. This is reported in Fig. 4(c): far into the NC, the distortion energy is negligible, but gets increasingly large upon approaching the interface, reaching a maximum and decreasing thereafter. Throughout the main oxide region, the average atomic energy does not show pronounced variations.

As a final observation concerning the structure, just as in the planar interface case, there is a large proportion of bridging bonds: for all NC sizes, nearly 90% of suboxide Si atoms have at least one bridging bond with other suboxides; all suboxides are present at the interface, with a majority of Si^{+3}, but Si-Si dimers are seldom found.

C. Discussion

The faceting of freestanding NCs results from the minimization of surface tension. The interfacial energy is therefore expected to play an important role in determining the equilibrium shape of embedded NCs. Experiments show that embedded NCs smaller than 50 Å are spherical, while larger ones develop well-defined facets.[6,8,13] Our calculations provide a rationale for these observations: from Fig. 3(a), we find that the interfacial energy for NCs smaller than 20 Å is lower than that of the corresponding planar interface, suggesting that spherical NCs are favored over faceted ones in this size range. The crossover diameter we find is, however, smaller than that observed in experiments; this is likely due to limitations of our approach—the exact nature and orientation of the interface is a delicate balance between numerous factors. Nevertheless, the behavior we observe is qualitatively correct and our calculations account for the experimental observations.

It has been observed that Si NCs grow with annealing time.[32,33] This might seem to be counterintuitive since the

interfacial energy increases with size. The relevant quantity, however, is the excess energy density, defined as $\rho=\Delta E/\Omega=6\gamma/D$, where $\Omega=\pi D^3/6$ is the volume of embedded NC. This is plotted in Fig. 3(d); indeed, the excess energy density decreases with size. Again, here, we find no difference between normal and twinned NCs. Twin planes are, however, observed in real NCs only at diameters larger than 60 Å; smaller NCs usually are defect-free.[8,14] We may speculate that there is some sort of kinetic barrier against twinning during nucleation and growth or that the barrier for an atom to diffuse from a twinning site to a normal site is so low that a normal state readily forms. Thus, all NCs would be "born" without defects; defects (such as twin planes) develop upon further growth, e.g., on coalescing with another NC. In fact, the coalescence of small Si NCs by twinning has been found experimentally to play an important role in the growth of large embedded Si NCs.[24,34]

IV. SUMMARY

We have used MC methods to investigate the interfacial properties between c-Si and a-SiO_2. Large embedded NCs are found to have higher interfacial energies than smaller ones; we also found that NCs larger than ~20 Å have interface energies larger than that of Si(111)[Si^{+1}]/a-SiO_2, which has the lowest energy among the different orientations examined. As a consequence, large NCs are faceted while small ones are spherical; the driving force for faceting is the minimization of the total interfacial energy. Finally, our calculations reveal no significant differences between normal and twinned NCs, suggesting that the experimentally observed stacking faults in large NCs might result from the coalescence of smaller defect-free NCs.

ACKNOWLEDGMENTS

We are indebted to G. Ross and F. Schiettekatte for useful discussions. L.T.K. wishes to thank G. Hadjisavvas for help in implementing the WWW algorithm. This work has been supported by grants from the Natural Sciences and Engineering Research Council of Canada (NSERC) and the Fonds Québécois de la Recherche sur la Nature et les Technologies (FQRNT). We are grateful to the Réseau Québécois de Calcul de Haute Performance (RQCHP) for generous allocations of computer resources.

*Corresponding author. laurent.lewis@umontreal.ca

[1] Y. Inoue, A. Tanaka, M. Fujii, S. Hayashi, and K. Yamamoto, J. Appl. Phys. **86**, 3199 (1999).
[2] S. Tiwari, F. Rana, H. Hanafi, A. Hartstein, E. F. Crabbe, and K. Chan, Appl. Phys. Lett. **68**, 1377 (1996).
[3] S. Huang, S. Banerjee, R. T. Tung, and S. Oda, J. Appl. Phys. **93**, 576 (2003).
[4] H. Takagi, H. Ogawa, Y. Yamazaki, A. Ishizaki, and T. Nakagiri, Appl. Phys. Lett. **56**, 2379 (1990).
[5] S. Cheylan and R. G. Elliman, Appl. Phys. Lett. **78**, 1912 (2001).
[6] Y. Ishikawa, N. Shibata, and S. Fukatsu, Appl. Phys. Lett. **68**, 2249 (1996).
[7] Y. Q. Wang, R. Smirani, and G. G. Ross, Nanotechnology **15**, 1554 (2004).
[8] Y. Q. Wang, R. Smirani, and G. G. Ross, Nano Lett. **4**, 2041 (2004).
[9] N. Daldosso, M. Luppi, S. Ossicini, E. Degoli, R. Magri, G. Dalba, P. Fornasini, R. Grisenti, F. Rocca, L. Pavesi, S. Boninelli, F. Priolo, C. Spinella, and F. Iacona, Phys. Rev. B **68**, 085327 (2003).
[10] M. Luppi and S. Ossicini, Phys. Rev. B **71**, 035340 (2005).
[11] G. Hadjisavvas and P. C. Kelires, Phys. Rev. Lett. **93**, 226104 (2004).
[12] G. Hadjisavvas, I. N. Remediakis, and P. C. Kelires, Phys. Rev. B **74**, 165419 (2006).
[13] Y. Q. Wang, R. Smirani, F. Schiettekatte, and G. G. Ross, Chem. Phys. Lett. **409**, 129 (2005).
[14] Y. Q. Wang, R. Smirani, and G. G. Ross, Appl. Phys. Lett. **86**, 221920 (2005).
[15] F. Wooten, K. Winer, and D. Weaire, Phys. Rev. Lett. **54**, 1392 (1985).
[16] S. von Alfthan, A. Kuronen, and K. Kaski, Phys. Rev. B **68**, 073203 (2003).
[17] G. T. Barkema and N. Mousseau, Phys. Rev. B **62**, 4985 (2000).
[18] R. L. C. Vink, G. T. Barkema, M. A. Stijnman, and R. H. Bisseling, Phys. Rev. B **64**, 245214 (2001).
[19] D. R. Hamann, Phys. Rev. B **61**, 9899 (2000).
[20] R. H. Byrd, P. Lu, and J. Nocedal, SIAM J. Sci. Comput. (USA) **16**, 1190 (1995).
[21] C. Zhu, R. H. Byrd, and J. Nocedal, ACM Trans. Math. Softw. **23**, 550 (1997).
[22] Y. Tu and J. Tersoff, Phys. Rev. Lett. **84**, 4393 (2000).
[23] A. Korkin, J. C. Greer, G. Bersuker, V. V. Karasiev, and R. J. Bartlett, Phys. Rev. B **73**, 165312 (2006).
[24] Y. Q. Wang, R. Smirani, G. G. Ross, and F. Schiettekatte, Phys. Rev. B **71**, 161310(R) (2005).
[25] P. J. Grunthaner, M. H. Hecht, F. J. Grunthaner, and N. M. Johnson, J. Appl. Phys. **61**, 629 (1987).
[26] J. H. Oh, H. W. Yeom, Y. Hagimoto, K. Ono, M. Oshima, N. Hirashita, M. Nywa, A. Toriumi, and A. Kakizaki, Phys. Rev. B **63**, 205310 (2001).
[27] F. J. Himpsel, F. R. McFeely, A. Taleb-Ibrahimi, J. A. Yarmoff, and G. Hollinger, Phys. Rev. B **38**, 6084 (1988).
[28] K. Ohishi and T. Hattori, Jpn. J. Appl. Phys., Part 2 **33**, L675 (1994).
[29] A. Pasquarello, M. S. Hybertsen, and R. Car, Phys. Rev. Lett. **74**, 1024 (1995).
[30] F. Giustino, A. Bongiorno, and A. Pasquarello, J. Phys.: Condens. Matter **17**, S2065 (2005).
[31] S. D. Kosowsky, P. S. Pershan, K. S. Krisch, J. Bevk, M. L. Green, D. Brasen, L. C. Feldman, and P. K. Roy, Appl. Phys. Lett. **70**, 3119 (1997).
[32] K. S. Min, K. V. Shcheglov, C. M. Yang, H. A. Atwater, M. L. Brongersma, and A. Polman, Appl. Phys. Lett. **69**, 2033 (1996).
[33] T. S. Iwayama, T. Hama, D. E. Hole, and I. W. Boyd, Surf. Coat. Technol. **158-159**, 712 (2002).
[34] Y. Q. Wang, R. Smirani, and G. G. Ross, J. Cryst. Growth **294**, 486 (2006).